g, 5.0 mmol) was added to a suspension of NaH (60% oil dispersion, 0.22 g, 5.5 mmol) in dry THF (10 mL) under N_2. After the mixture was stirred for 20 min, 1-(2-(*p*-toluenesulfonoxy)ethoxy)anthracene-9,10-dione (1.06 g, 2.5 mmol) was added as a solid. The reaction mixture was brought to reflux temperature and stirred for 18 h. The mixture was cooled and concentrated in vacuo. The residue was added to H_2O (25 mL) and extracted with $CHCl_3$ (2 × 25 mL). The combined organic phases were washed with brine (10 mL), dried ($MgSO_4$), and concentrated in vacuo. Column chromatography (90 g silica gel 60, 60% $CHCl_3$/hexanes–2% MeOH/$CHCl_3$) followed by recrystallization (EtOH) gave **5** (160 mg, 14%) as a yellow powder: mp 48–49 °C; ^1H NMR ($CDCl_3$) 3.33 (s, 3 H, CH_3), 3.55–4.05 (m, 18 H, CH_2's), 4.27 (t, 2 H, CH_2OAr), 7.22–8.22 (m, 7 H, Ar); IR (KBr) 1670, 1590, 1320, 1270, 1150, 1140, 1105, 990, 720 cm^{-1}. Anal. Calcd for $C_{25}H_{30}O_8$: C, 65.48; H, 6.61. Found: C, 66.64; H, 6.34.

1,8-Bis(1-oxaanthracene-9,10-dione)-3,6-dioxaoctane (6). Method A. Compound **6** was prepared from the potassium salt of 1-hydroxyanthraquinone (2.62 g, 0.01 mol), 1,2-bis(2-iodoethoxy)ethane (1.85 g, 0.005 mol), 18-crown-6 (2.64 g, 0.01 mol), and CH_3CN (30 mL) by a method analogous to that for the preparation of **7** (see procedure below). Column chromatography (silica gel 60, 2% MeOH/$CHCl_3$) followed by recrystallization (2-butanone) gave **6** (0.85 g, 30%) as a yellow powder: mp 173–175 °C; ^1H NMR ($CDCl_3$) 3.90, 4.03, and 4.30 (s, t, and t, 12 H, CH_2's), 7.24–8.24 ppm (m, 14 H, Ar); IR (KBr) 1670, 1590, 1325, 1275, 715 cm^{-1}. Anal. Calcd for $C_{34}H_{26}O_8$: C, 72.58; H, 4.67. Found: C, 72.48; H, 4.71.

Method B. Triethylene glycol (3.75 g, 25 mmol) was slowly added to a vigorously stirred suspension of NaH (60% oil dispersion, 2.7 g, 68 mmol) in dry THF (40 mL) under N_2. After the mixture was stirred for 45 min, 1-chloroanthraquinone (12.13 g, 50 mmol) was added as a solid, and the flask was rinsed with dry THF (20 mL). The reaction mixture was brought to reflux temperature and vigorously stirred for 6 h. The mixture was cooled and concentrated in vacuo. The residue was added to H_2O (300 mL) and extracted with $CHCl_3$ (300 mL then 100 mL). The combined organic phases were washed with brine (100 mL), dried ($MgSO_4$), and concentrated in vacuo. Two recrystallizations (2-butanone) gave **6** (9.3 g, 66%) as a yellow powder (mp 146–148 °C solidifies and remelts at 175–177 °C). An analytically pure sample was obtained by passing 1 g of sample through a column of silica gel 60 (20 g, 2% MeOH/$CHCl_3$) followed by recrystallization (CH_3CN). Approximately 0.97 g of sample was recovered (mp 170–173 °C) which had physical properties identical with those reported above.

(Hydroxymethyl)-15-crown-5 was prepared as previously described[14] in 39% overall yield. The product had physical properties identical with those reported.

Preparation of 1-((1-Oxaanthracene-9,10-dione)methyl)-15-crown-5 (7). Method A. To a refluxing acetonitrile solution (20 mL) containing the potassium salt of 1-hydroxyanthraquinone (KHA, see above, 2.39 g, 9.1 mmol) and 18-crown-6 (2.41 g, 9.1 mmol) was added hydroxymethyl-15-crown-5 *p*-toluenesulfonate (2.5 g, 6.2 mmol) in acetonitrile (20 mL). After addition the reaction was heated at reflux for 3 days. After cooling, $CHCl_3$ (50 mL) and 3 N HCl (50 mL) were added. The phases were separated, and the aqueous portion was extracted with $CHCl_3$ (50 mL). The combined organic phases were washed with H_2O (25 mL) and brine (25 mL), dried ($MgSO_4$), and concentrated in vacuo. Column chromatography (silica gel 60, $CHCl_3$–5% MeOH/$CHCl_3$) gave an oil which crystallized on standing. The resulting solid was washed with EtOH to give **7** (1.1 g, 39%) as a yellow solid: mp 100–102 °C; ^1H NMR ($CDCl_3$) 3.68–4.22 (m, 21 H, aliphatic), 7.29–8.30 ppm (m, 7 H, Ar); IR (KBr) 1670, 1590, 1325, 1125, 715 cm^{-1}. Anal. Calcd for $C_{25}H_{28}O_8$: C, 65.77; H, 6.19. Found: C, 65.84; H, 6.24.

Method B. Hydroxymethyl-15-crown-5 (5.01 g, 20 mmol) in dry THF (15 mL) was slowly added to a vigorously stirred suspension of NaH (60% oil dispersion, 1.2 g, 30 mmol) in dry THF (15 mL) under N_2. After the mixture was stirred for 30 min, 1-chloroanthraquinone (4.85 g, 20 mmol) was added as a solid, and the flask was rinsed with dry THF (20 mL). The reaction was stirred at ambient temperature for 18 h and concentrated in vacuo. The residue was added to $CHCl_3$ (100 mL) and H_2O (50 mL). The phases were separated, and the aqueous portion was extracted with $CHCl_3$ (100 mL). The combined organic phases were washed with brine (50 mL), dried ($MgSO_4$), and concentrated in vacuo. Column chromatography (230 g, silica gel 60, 60% $CHCl_3$/hexanes–$CHCl_3$) followed by crystallization of the oily residue in EtOH gave **7** (3.6 g, 40%) with physical properties identical with those obtained by using method A.

Acknowledgment. We thank the National Institutes of Health for Grants (GM-31846, GM-33940, and GM-36262) and W. R. Grace & Co. which supported this work.

Registry No. 1, 82-39-3; **2**, 104779-00-2; **3**, 104779-01-3; **4**, 104549-31-7; **5**, 104779-02-4; **6**, 104779-03-5; **7**, 104084-69-7; HA, 129-43-1; KHA, 26035-17-6; Li^+, 17341-24-1; Na^+, 17341-25-2; K^+, 24203-36-9; diethylene glycol monomethyl ether, 111-77-3; 1-chloroanthraquinone, 82-44-0; triethylene glycol monomethyl ether, 112-35-6; tetraethylene glycol monomethyl ether, 23783-42-8; 1-(2-hydroxyethoxy)anthracene-9,10-dione, 38933-94-7; 1-(2-(*p*-tolylsulfonoxy)ethoxy)anthracene-9,10-dione, 104779-04-6; 1,2-bis(2-iodoethoxy)ethane, 36839-55-1; triethylene glycol (hydroxymethyl)-15-crown-5-*p*-toluenesulfonate, 84131-00-0; (hydroxymethyl)-15-crown-5, 75507-25-4; ethylene carbonate, 96-49-1.

(14) Dishong, D. M.; Diamond, C. J.; Cinoman, M. I.; Gokel, G. W. *J. Am. Chem. Soc.* **1983**, *105*, 586.

Unusually Facile Dissociation of Benzene by Ruthenium Metal

J. A. Polta and P. A. Thiel*

Contribution from the Department of Chemistry and Ames Laboratory, Iowa State University, Ames, Iowa 50011. *Received July 16, 1986*

Abstract: Associative chemisorption of benzene at room temperature has been reported on several group VIII metal surfaces (Ni, Rh, Pd, Pt), where molecular adsorption is followed by partial dissociation and partial desorption at higher teperatures. However, we find that between one-fourth and one-half of a full layer of benzene adsorbs *irreversibly at 85 K* into a state which represents either a dissociated form of benzene or a molecular precursor to dissociation. Those molecules which subsequently adsorb do not dissociate and can desorb in several states between 120 and 180 K. For these, the chemisorption bond is very weak, only 9–11 kcal/mol. We propose that this is true because the Ru surface is electronically or sterically modified by the dissociative phase. Coadsorbed water can prevent decomposition but cannot displace benzene from the dissociative phase. Furthermore, the adsorbed benzene surface layer acts as a template for growth of a metastable benzene multilayer, which has a heat of sublimation of 7 ± 1.4 kcal/mol. The metastable multilayer is eventually converted completely to normal bulk benzene at very high coverages. The data are obtained from several types of experiments: multiple-mass thermal desorption spectroscopy of benzene itself, quantitative oxidation of residual carbon, and competitive coadsorption of benzene and water.

(I) Introduction

There is a large body of literature which describes the chemisorption of benzene on low-index, single-crystal surfaces of Ni, Rh, Pd, and Pt.[1-17] These studies have generally dealt with a saturated chemisorbed layer at room temperature, and certain conclusions are common to all of them: (1) Benzene adsorbs

(1) Demuth, J. E.; Eastman, D. E. *Phys. Rev. Lett.* **1974**, *32*, 1123.

0002-7863/86/1508-7560$01.50/0

without dissociation at 300 K. (2) The molecular plane is parallel to the surface, and the adsorption bond involves benzene's π electrons. (3) Molecular desorption occurs at 400–550 K. (4) Dissociation accompanies desorption to varying degrees.

We find that ruthenium is unusual in that there is a very low effective barrier for benzene dissociation compared with the metals cited above. This property is important for understanding heterogeneous reactions catalyzed by Ru in which benzene is a reactant or product.

The adsorption of benzene on Ru(001) has been studied previously by two groups.[18,19] Shanahan and Muetterties[18] noted that benzene on Ru(001) was unusual in that the molecule could not be displaced by PF_3 or $P(CH_3)_3$ at 300 K, and molecular desorption was absent above 300 K. Both findings were indirect indications of dissociative adsorption. In an earlier study, however, Kelemen and Fisher[19] had used ultraviolet photoemission data to argue that adsorption occurs without dissociation at 300 K, much like other metals. In the present work, we have used thermal desorption spectroscopy to quantitatively measure the amount of benzene which dissociates, the way in which the dissociative state influences other states which desorb molecularly, and the extent to which coadsorption of water can inhibit dissociation. This represents the most complete study of benzene adsorption at a ruthenium single-crystal surface to date. We provide evidence that between one-half and one-fourth of a full benzene layer dissociates, or irreversibly forms a molecular precursor to dissociation, even at 85 K.

(II) Experimental Methods

The experiments were performed in an ultrahigh vacuum (UHV) apparatus with a typical base pressure of 1×10^{-10} Torr (1 Torr ≡ 133.3 Nm^{-2}). The Ru(001) sample, ca. 1 cm^2 in area, was grown at the Ames Laboratory Materials Preparation Center. It was oriented and polished to within 0.5 deg of the (001) face on both sides. Sulfur and silicon were the major contaminants and were removed by successive heating, ion bombardment, and oxidation cycles, similar to the procedure described by Williams and Weinberg.[20] The sample was mounted by spot-welding to two 0.020-in.-diameter Ta wires. The wires were attached to a liquid-nitrogen-coolable cold finger and were used to resistively heat the sample.[21] A W–5% Re vs. W–26% Re thermocouple was spotwelded to the top edge of the sample.

Both water (triply distilled) and benzene were purified by repeated freeze–thaw cycles under vacuum. The sample was exposed to water by backfilling the entire UHV chamber. Water exposures are reported in units of langmuirs (1 langmuir ≡ 1×10^{-6} Torr·s). Benzene was introduced via a directed capillary-array doser.[22] Benzene exposures are reported in units of langmuir equivalents, obtained by comparing exposures of CO through the doser with exposures from backfilling the chamber. For both benzene and water, no correction has been made for ionization gauge sensitivities in the reported exposures. Unless otherwise noted, the extent of carbon remaining on the surface after each experiment was measured by exposing the sample to 50 langmuirs of oxygen and monitoring the partial pressure of CO, mass 28, while heating the sample. This procedure was done twice after each experiment to ensure the total quantitative removal of carbon. The sample was held at 85 K during gas exposures. Partial pressures of gases with different molecular weights were monitored, effectively simultaneously, as functions of time and sample temperature with a PDP 11/23 microcomputer interfaced to an EAI 250 quadrupole mass spectrometer and an independent temperature controller.[23] The sample was in direct line-of-sight and about 8 cm removed from the mass spectrometer ionizer. The heating rate was 0.10 mV s^{-1}, which corresponds to an actual temperature change of 9 to 12 K s^{-1} in the region of benzene desorption, 120–180 K.

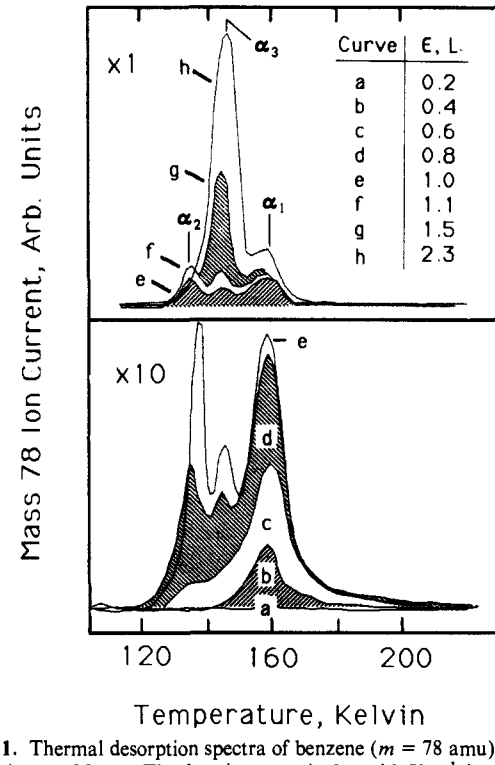

Figure 1. Thermal desorption spectra of benzene (m = 78 amu) following adsorption at 85 K. The heating rate is 9 to 12 K s^{-1} in the range 120–180 K.

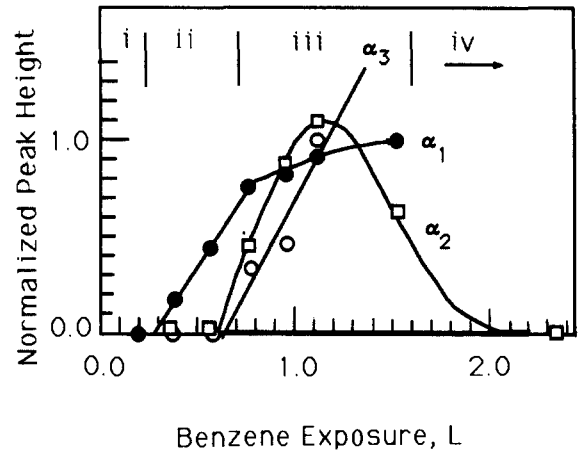

Figure 2. Height of each benzene desorption peak as a function of benzene exposure to clean ruthenium at 85 K. The heights are normalized to that of the α_1 state at 1.5 langmuirs.

(2) Bertolini, J. C.; Dalmai-Imelik, G.; Rousseau, J. *Surf. Sci.* **1977**, *67*, 478. Also: Bertolini, J. C.; Rousseau, J. *Surf. Sci.* **1979**, *89*, 467.
(3) Lloyd, D. R.; Quinn, C. M.; Richardson, N. V. *Solid State Commun.* **1977**, *23*, 141.
(4) Lehwald, S.; Ibach, H.; Demuth, J. E. *Surf. Sci.* **1978**, *78*, 577.
(5) Friend, C. M.; Muetterties, E. L. *J. Am. Chem. Soc.* **1981**, *103*, 773.
(6) Tsai, M.-C.; Friend, C. M.; Muetterties, E. L. *J. Am. Chem. Soc.* **1982**, *104*, 2539.
(7) Koel, B. E.; Somorjai, G. A. *J. Electron Spectrosc. Rel. Phenom.* **1983**, *29*, 287.
(8) Koel, B. E.; Crowell, J. E.; Mate, C. M.; Somorjai, G. A. *J. Phys. Chem.* **1984**, *88*, 1988.
(9) Nyberg, G. L.; Richardson, N. V. *Surf. Sci.* **1979**, *85*, 335.
(10) Hofmann, P.; Horn, K.; Bradshaw, A. M. *Surf. Sci.* **1981**, *105*, L260.
(11) Gentle, T. M.; Muetterties, E. L. *J. Phys. Chem.* **1983**, *87*, 2469.
(12) Sesselmann, W.; Woratschek, B.; Ertl, G.; Küppers, J.; Haberland, H. *Surf. Sci.* **1983**, *130*, 245.
(13) Netzer, F. P.; Mack, J. U. *J. Phys. Chem.* **1983**, *79*, 1017.
(14) Kesmodel, L. L. *Phys. Rev. Lett.* **1984**, *53*, 1001.
(15) Waddill, G. D.; Kesmodel, L. L. *Phys. Rev. B* **1985**, *31*, 4940.
(16) Fischer, T. E.; Kelemen, S. R.; Bonzel, H. P. *Surf. Sci.* **1977**, *64*, 157. Fischer, T. E.; Kelemen, S. R. *J. Catal.* **1978**, 24.
(17) Tsai, M.-C.; Muetterties, E. L. *J. Am. Chem. Soc.* **1982**, *104*, 2534. Tsai, M.-C.; Stein, J.; Friend, C.-M.; Muetterties, E. L. *J. Am. Chem. Soc.* **1982**, *104*, 3533.
(18) Shanahan, K. L.; Muetterties, E. L. *J. Phys. Chem.* **1984**, *88*, 1996.
(19) Kelemen, S. R.; Fischer, T. E. *Surf. Sci.* **1981**, *102*, 45.
(20) Williams, E. D.; Weinberg, W. H. *Surf. Sci.* **1979**, *82*, 93.
(21) Thiel, P. A.; Anderegg, J. W. *Rev. Sci. Instrum.* **1984**, *55*, 1669.
(22) Goodman, D. W.; Madey, T. E.; Ono, D. M.; Yates, J. T., Jr. *J. Catal.* **1977**, *50*, 279.
(23) Herz, H.; Conrad, H.; Kuppers, J. *J. Phys. E.* **1979**, *12*, 369.

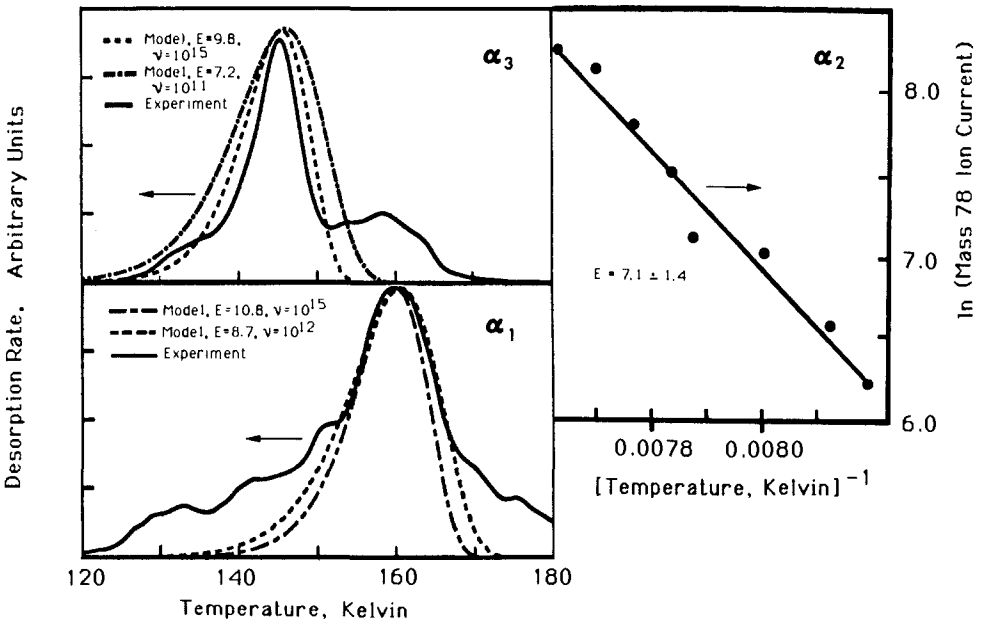

Figure 3. Kinetic models of benzene thermal desorption states. Desorption energies (E) are given in kcal/mol, and pre-exponential rate factors (ν) are given in s^{-1}. The mass 78 ion current is proportional to the desorption rate. α_1: The experimental benzene desorption spectrum is shown by the solid line, following an exposure of 0.6 langmuir at 85 K. The dashed lines show two calculated spectra. α_2: Logarithm of the benzene desorption rate in the α_2 state as a function of reciprocal temperature, following a benzene exposure of 0.8 langmuir. The line is a least-squares fit to the data. The slope indicates a heat of desorption (sublimation) of 7.1 ± 1.4 kcal/mol, where the uncertaintly reflects one standard deviation for the least-squares fit. α_3: The experimental benzene desorption spectrum is shown by the solid line, following an exposure of 1.5 langmuirs at 85 K. The dashed lines show two calculated spectra.

(III) Experimental Results

(1) Desorption of Molecular Benzene. A minimum exposure of benzene (0.2 langmuir) is necessary to detect any molecular desorption. This is due to complete and irreversible decomposition of benzene below this exposure, as will be discussed in the following section.

Figure 1 illustrates the thermal desorption spectra of molecular benzene following various exposures to clean Ru(001) at 85 K. The spectra feature three distinct molecular desorption states at 130, 145, and 160 K. We shall refer to these states as α_2, α_3, and α_1, respectively, where the subscripts have been chosen to correspond to the order in which the states are filled.

The 160 K state (α_1) appears first, growing with increasing exposure until it saturates at about 0.7 langmuir. Its development in this exposure regime is also illustrated in Figure 2. The peak temperature and half-width of the α_1 state are constant with increasing coverage, indicating first-order kinetics. Furthermore, models of the experimental peak assuming first-order desorption kinetics yield reasonable parameters: a desorption barrier of 8.7–10.8 kcal/mol and a pre-exponential rate factor of 10^{12}–10^{15} s^{-1}. The range in values reflects allowance for possible broadening of the experimental peak which, in our judgment, may be as large as 4 K. This could be due to overlap with other peaks and to experimental artifacts, such as sample inhomogeneity or thermal gradients. The models are illustrated in Figure 3.

The α_2 state, which first appears at 130 K and after 0.7 langmuir exposure, is populated after the α_1 state but prior to the α_3 state (at 145 K). This is unusual, because binding energy is a strong function of desorption temperature, and so desorption states are usually populated sequentially from high temperature to low temperature as coverage increases. Furthermore, Figures 1 and 2 illustrate that the α_2 state is only observed in the intermediate coverage regime; α_2 completely disappears at about 1.5 langmuirs. This state exhibits zero-order kinetics at all coverages, because the leading edge overlaps for spectra with different coverage and constant heating rate (Figure 1) and also for spectra with constant coverage and different heating rate (Figure 4). Evaluation of the leading edge, assuming zero-order desorption kinetics, indicates that the binding energy of this state is 7.1 ± 1.4 kcal/mol. The results of the modelling are shown in Figure 3.

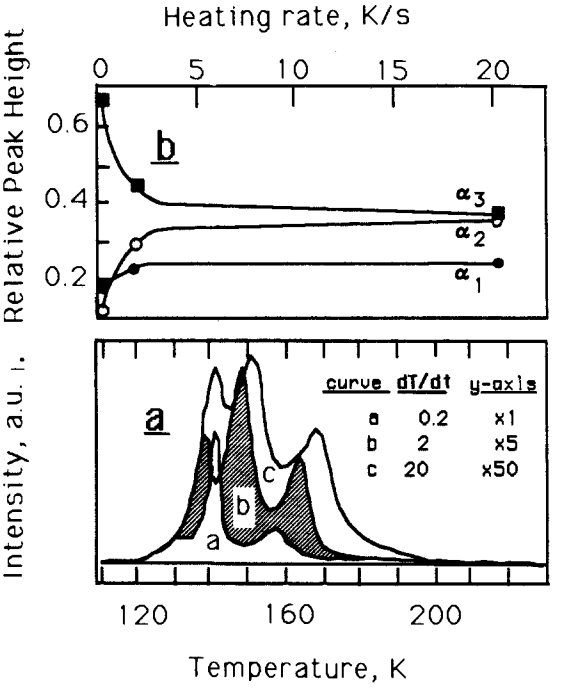

Figure 4. (a) Thermal desorption spectra of benzene at various heating rates, following constant exposure of 0.9 langmuir of benzene to clean Ru at 85 K. The heating rate, dT/dt, is given in K s^{-1}. (b) Peak height of each individual desorption feature, relative to the sum of all three peak heights, as a function of heating rate for the spectra of part a.

Further information on the nature of the α_2 state is provided by variation of the heating rate (dT/dt) during thermal desorption, as shown in Figure 4a. At the slowest heating rate (curve a), the α_3 state dominates the spectrum, whereas at the fastest heating rate (curve c), α_2 and α_3 are of comparable intensity. Decomposition does not complicate the desorption processes illustrated in Figure 4, as we will discuss in the following section. The relative heights of the three peaks are shown as functions of heating rate in Figure 4b. These data show that the α_2 state can convert to the α_3 state during the desorption ramp, possibly by molecular

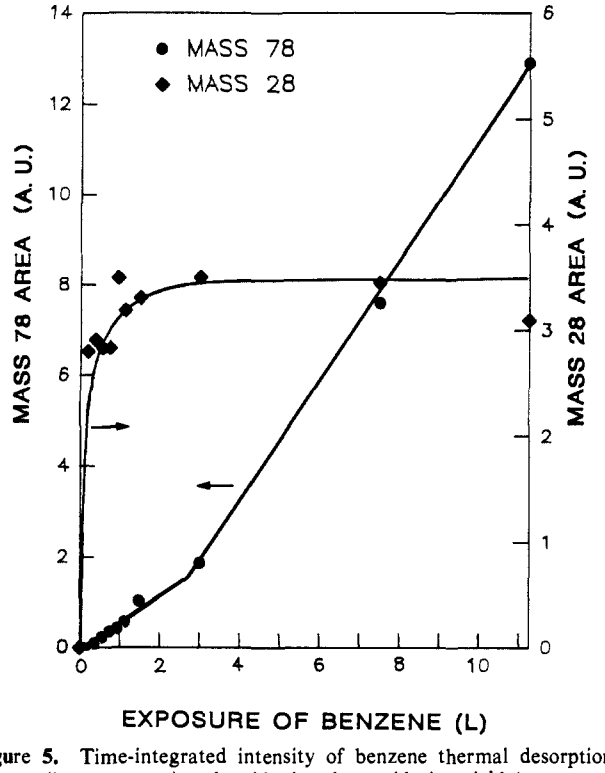

Figure 5. Time-integrated intensity of benzene thermal desorption spectra (bottom curve) and residual carbon oxidation yield (top curve) as functions of benzene exposure at 85 K.

reorientation or by diffusion over the surface. (To a much smaller extent, some conversion from the α_1 to the α_3 state may also occur.) Therefore the α_2 state represents molecules which are indeed less stable than α_3 molecules, as the desorption peak temperatures suggest, but the α_2 molecules can be kinetically trapped.

The mid-temperature state, at 145 K (α_3), populates last and does not saturate. Because of the latter property, this must represent sublimation of bulk benzene, which is expected to exhibit zero-order desorption kinetics. The α_3 state first appears at exposures above 0.7 langmuir, as shown in Figures 1 and 2. Between 0.7 and 1.5 langmuirs of exposure, the peak temperature of the α_3 state shifts upward slightly with increasing coverage, yet the leading edges of peaks at different coverages do not overlap. In a simple picture, this indicates that the desorption kinetics are somewhere between zero-order and first-order. Futhermore, attempts to model this peak for exposure below 1.5 langmuirs, assuming first-order kinetics and physically reasonable kinetic parameters, are not successful, as shown in Figure 3. The experimental peak is anomalously narrow, which is also consistent with desorption kinetics which are fractional-order. (Experimental artifacts, such as inhomogeneous sample heating, would all tend to *broaden* the observed peak.) At exposures between 0.7 and 1.5 langmuirs, we attribute the α_3 state to desorption from small islands of condensed benzene. At exposures of 1.5 langmuirs and above, the desorption kinetics converge to zero-order because the leading edges increasingly overlap, as shown in Figure 1b. We therefore ascribe the α_3 state at large exposures (above 1.5 langmuirs) to normal sublimation of bulk-phase benzene, with a heat of sublimation of 10.4 kcal/mol.[26] Transitions from fractional-order to zero-order desorption kinetics have also been observed and discussed for other systems, such as Xe on W, in which multilayers grow starting from small islands.[24,25]

From Figure 2, it appears that there are four main regimes of benzene exposure. The first (i), below 0.2 langmuir, is where no desorption of molecular benzene occurs. The second (ii), up to about 0.7 langmuir, is the regime where only the α_1 state appears.

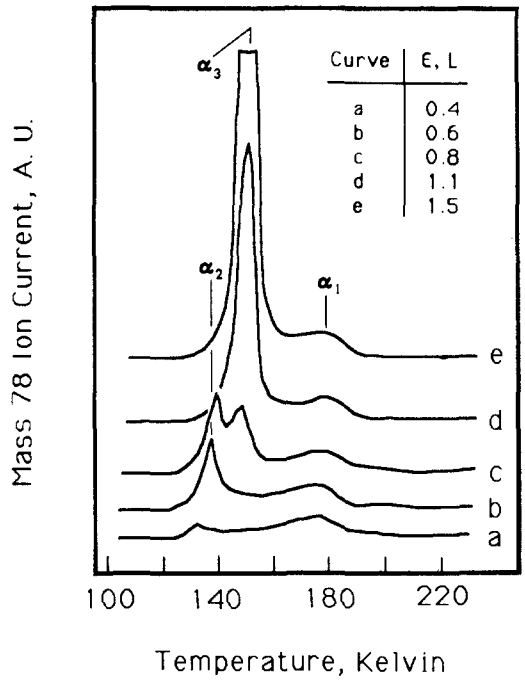

Figure 6. Thermal desorption spectra of benzene (m = 78 amu) following exposure to a residue-covered surface at 85 K. The surface was not cleaned between successive experiments but only heated to 300 K.

In the third (iii), between ca. 0.7 and 1.5 langmuirs, the rate of filling of the α_1 state decreases and the other two states, α_2 and α_3, grow simultaneously. However, α_2 dominates α_3 in this regime. Finally, above 1.5 langmuirs (iv), the α_2 state diminishes to zero while α_3 continues to grow. Some of these events are reflected also in the time-integrated benzene peak intensity as a function of exposure, shown in Figure 5. The transition between the first and second regimes is evident, and it also appears that the adsorption probability increases between about 2 and 3 langmuirs, which correlates with the development of true bulklike characteristics in the α_3 state. The formation of the benzene multilayer apparently enhances the sticking coefficient slightly.

Further information on the nature of the adsorption states is obtained from the data shown in Figure 6, where the Ru surface was first covered with benzene adsorption products and then used as a substrate for normal adsorption–desorption experiments. It was not cleaned in oxygen between successive experiments, but only heated each time to 300 K. Comparison of Figure 1, curve c, with Figure 6, curve b, shows a significant increase in the maximum α_2:α_1 intensity ratio, by about a factor of 3. Note that the spectra of Figure 6 exhibit similar peak temperatures, desorption characteristics, and sequence of filling of states as shown in Figure 1. The exception to this statement is the peak temperature of the α_1 state, which is shifted upward by 20 K relative to Figure 1.

We propose a model for the three desorption states of molecular benzene which is illustrated in Figure 7. The stages of exposure are the same as those defined in Figure 2. In the first stage, benzene must either decompose or form a precursor to dissociation. For the sake of discussion, we shall identify this as β-benzene. This occurs irreversibly *prior to* desorption of molecular benzene, as we shall discuss in the following sections.

After stage i, the α_1 state fills in stage ii. The adsorption enthalpy of the α_1 molecules is 8.7–10.8 kcal/mol. We propose that the α_1 state represents molecules adsorbed at the metal surface but strongly influenced by coadsorbed β-benzene for these reasons: (1) it displays simple first-order desorption kinetics (Figures 1 and 3); (2) it is suppressed, relative to α_2, by preadsorbed β-benzene (Figure 6); and (3) it cannot be populated until a certain minimum amount of the β-phase has been filled (Figure 5).

We propose that β-benzene exerts a steric or electronic influence on the coadsorbed α_1 molecules. It may be, for instance, that after all the dissociation sites are filled, patches of open metal remain

(24) Redondo, A.; Zeiri, Y.; Goddard, W. A., III *Surf. Sci.* **1984**, *136*, 41.
(25) Opila, R.; Gomer, R. *Surf. Sci.* **1981**, *112*, 1.
(26) Wyckoff, R. W. G. *Crystal Structures*; Interscience: New York, 1963; Vol. 6, pp 1–2.

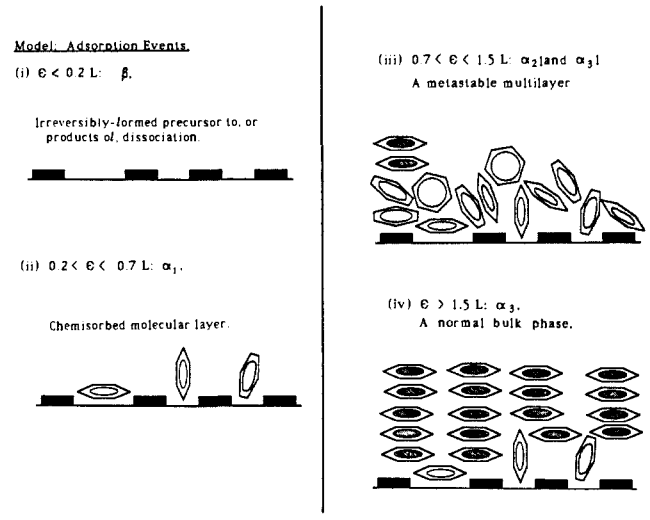

Figure 7. Model for adsorption of benzene on Ru(001). The four stages of adsorption correspond to those designated in Figure 2. The molecules in the normal bulk phase are shaded; their arrangement in the figure does *not* reflect the true arrangement of molecules in the crystal.[26]

at which the α_1 molecules can adsorb, not with their planes parallel to the metal but in less favorable positions, as shown in Figure 7ii. The interaction with the metal in this way is not sufficient to cause the molecule to dissociate. Alternatively, it may be that the α_1 state represents molecules which adsorb parallel to open patches of Ru surface, but which do not dissociate because the electronic properties of the metal are heavily modified by the coadsorbed β-benzene. This possibility is also shown in Figure 7ii. In any case, we do not propose that the α_1 state represents a mixture of widely different kinds of molecules, since it is a single well-defined desorption peak and obeys reasonable first-order kinetic parameters. One of the possibilities shown in Figure 7ii may be correct, but probably not all.

In the third adsorption phase, α_2 grows and then declines; the α_3 state grows simultaneously. We propose that the α_2 state represents molecules which form a metastable multilayer strongly influenced by the β surface layer, consistent with the following observations: (1) the α_2 state displays zero-order desorption kinetics (Figures 1, 3, and 4); (2) it is enhanced (relative to α_1) by preadsorbed β-benzene or its products (Figure 6); (3) $\alpha_2 \rightarrow \alpha_3$ conversion is assisted by slower heating rates (Figure 4); and (4) the α_2 state only appears in a narrow coverage range (Figures 1 and 2). In our model, the β-benzene adlayer serves as a template for growth of an α_2-multilayer, in which the molecules cannot interact with each other as favorably as in normal bulk benzene, making this anomalous multilayer (α_2) less stable than the true multilayer (α_3). The heat of sublimation of the α_2 molecules is 7.1 ± 1.4 kcal/mol. Finally, in stage iv, the stable bulk multilayer (α_3) is formed and the metastable multilayer (α_2) declines. It may be that as coverage increases, small seeds of the true multilayer form (indicated with shaded hexagons in Figure 7iii). These could serve as nucleation sites to convert the rest of the metastable multilayer to its more stable structure. Alternatively, it is possible that the α_2 state is physically sandwiched between the α_3 and surface layers and is thereby prevented from desorbing at high coverages until after the α_3 state is gone. It could therefore be forced to desorb at higher temperatures without necessarily undergoing $\alpha_2 \rightarrow \alpha_3$ conversion. Both possibilities would account for the *disappearance* of the α_2 state with increasing coverage.

The structure of solid benzene is known to be one in which the benzene molecules are packed in an orthorhombic structure.[26] We believe that this corresponds to the α_3 state, with a heat of sublimation of 10.4 kcal/mol.[27] The α_3 state displays fractional-order desorption kinetics at low coverage but changes to zero-order kinetics at high coverage (Figures 1 and 3).

(27) Weast, R. C., Ed. *Handbook of Chemistry and Physics*, 61st ed.; CRC: Boca Raton, 1980.

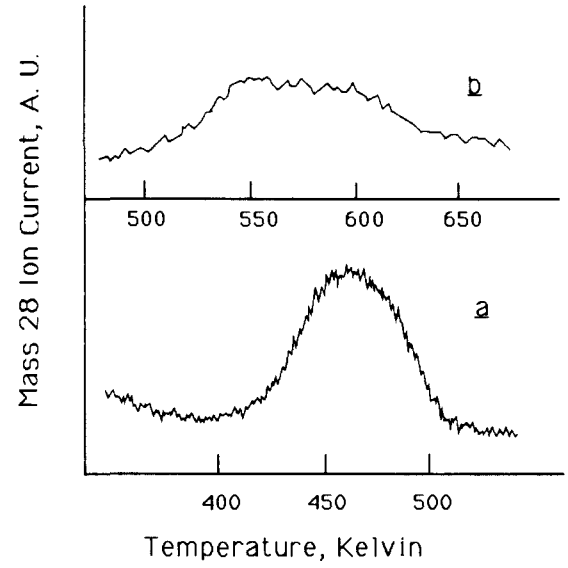

Figure 8. (b) Thermal desorption of CO following oxygen exposure to a Ru surface covered with residues from benzene decomposition. The benzene exposure was 3.8 langmuirs. (a) Thermal desorption of CO following 0.5 langmuir of CO exposure to clean Ru at 300 K.

(2) Decomposition of Benzene. The extent of benzene decomposition was measured quantitatively by adsorbing oxygen and recording the thermal desorption spectrum of CO (28 amu) after desorption of molecular benzene. Mass 44, CO_2, represented less than 1% of the integrated CO peak intensity. A typical set of data is shown in Figure 8, where the CO desorption after carbon oxidation (curve a) is compared with CO from deliberate exposure of CO to clean Ru (curve b). The total amount of desorbing CO is the same in both spectra. Carbon oxidation, on Ru and other metals (e.g., ref 28 and 29) results in CO desorption at higher temperature than for molecularly adsorbed CO; this is because the rate of CO desorption from carbon oxidation is reaction-limited.[28,29] In our experiments, the temperature difference is 100 to 150 K, as shown. The benzene which decomposes to oxidizable carbon is β-benzene.

The amount of CO obtained from carbon oxidation is shown as a function of benzene exposure in the top curve of Figure 5. The maximum amount of carbon is obtained after exposures of 1 langmuir or greater, and 70% of this limiting value is reached already after exposures of 0.2 langmuir. In other words, most of the dissociation occurs within stage i of Figure 2, but some additional decomposition continues during stage ii.

The maximum amount of carbon obtained from oxidation corresponds to 0.3 ± 0.1 monolayer of CO [assuming that the saturation coverage of CO on clean Ru is 0.65 monolayer[20]], which is equivalent to 0.05 ± 0.02 monolayer of benzene. [One monolayer is here defined as one adsorbate molecule per surface Ru atom ≡ 1.57×10^{15} molecules cm^{-2} on Ru(001).] It is thus reasonable that benzene decomposition is complete after only 1 langmuir of exposure, which is a total flux of about 0.15 monolayer. (There is an uncertainty of ca. ±0.08 monolayer in total flux due to uncertainty in ionization gauge calibration.)

The molecular dimensions of benzene are very close to those of cyclohexane,[30] and so previous estimates of absolute cyclohexane coverage in a filled layer[31] can be used also for benzene. The lower limit of 0.10 monolayer is obtained by assuming random, immobile, site-specific adsorption on the Ru lattice,[32] whereas the upper limit of 0.18 monolayer is obtained in the case of perfect, non-site-specific packing which is limited only by the molecular van der

(28) Madden, H. H.; Ertl, G. *Surf. Sci.* **1973**, *35*, 211.
(29) Schincho, E.; Egawa, C.; Naito, S.; Tamaru, K. *Surf. Sci.* **1985**, *155*, 153.
(30) Gavezzotti, A.; Simonetta, M.; Van Hove, M. A.; Somorjai, G. A. *Surf. Sci.* **1985**, *154*, 109.
(31) Polta, J. A.; Flynn, D. K.; Thiel, P. A. *J. Catal.* **1986**, *99*, 88.
(32) Sanders, D., private communication.

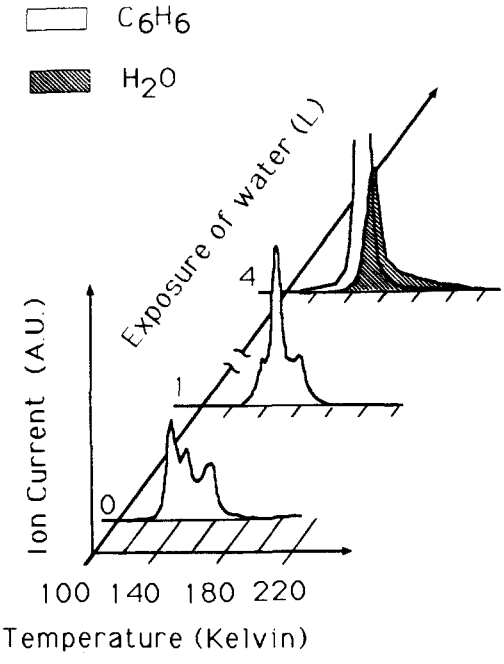

Figure 9. Thermal desorption spectra of benzene (open areas) and water (filled area) following coadsorption at 85 K. The water exposure occurs first and benzene second. Water exposures are varied; benzene is constant at 0.9 langmuir.

Waals radius.[31] [This upper limit is in very good agreement with the absolute coverage of a full layer of benzene on Pt(100), measured by Fischer et al.[16]] The total number of benzene molecules which dissociate on Ru(001), 0.05 monolayer, therefore represents approximately one-half to one-fourth of all the benzene molecules which could adsorb in a first layer.

The β-state may represent either benzene which is already dissociated at 85 K or that which is a strongly chemisorbed, molecular precursor to dissociation. From our data, we only know that elemental carbon is present by ca. 550 K, at which point it can be oxidized to CO. Also, molecular hydrogen desorbs between 450 and 500 K after benzene decomposition. The thermal desorption spectrum is similar to that for clean Ru(001), indicating that C–H bond cleavage does not limit the rate of H_2 desorption. The thermal desorption states of molecular benzene are rather insensitive to whether the surface was initially clean before adsorption or whether it was prepared by heating a benzene-covered surface to 300 K (Figure 6). This suggests that the chemical composition of the surface layer is the same or similar in both cases. The possible identity of the β-benzene will be discussed in section IV.

Formation of β-benzene does not compete with desorption in the α-states, following adsorption at 85 K. This is true because the yield of oxidized carbon is not influenced by variations in heating rate, within the range shown in Figure 4, although the variation in dT/dt strongly changes the distribution of benzene among the molecular desorption states. This suggests that β-benzene formation is independent of molecular desorption and probably precedes it; this conclusion is supported also by the results of experiments with coadsorbed water, described in the following section.

Finally, exposure of benzene to clean Ru(001) at 300 K results only in benzene decomposition. There is no molecular desorption at higher temperatures following adsorption at 300 K, in agreement with previous work by Shanahan and Muetterties.[18]

(3) Influence of Coadsorbed Water. The effect of pre-adsorbed water is shown in Figures 9 and 10. Figure 9 shows benzene TD spectra (78 amu, open areas) following constant benzene exposures of 0.9 langmuir; the pre-exposure to water is varied. The desorption of water (18 amu) is shown by the filled area. Figure 9 illustrates that water suppresses both the α_1 and α_2 states while enhancing the α_3 state. This is consistent with the interpretation we have described previously for α_1 and α_2, because water blocks

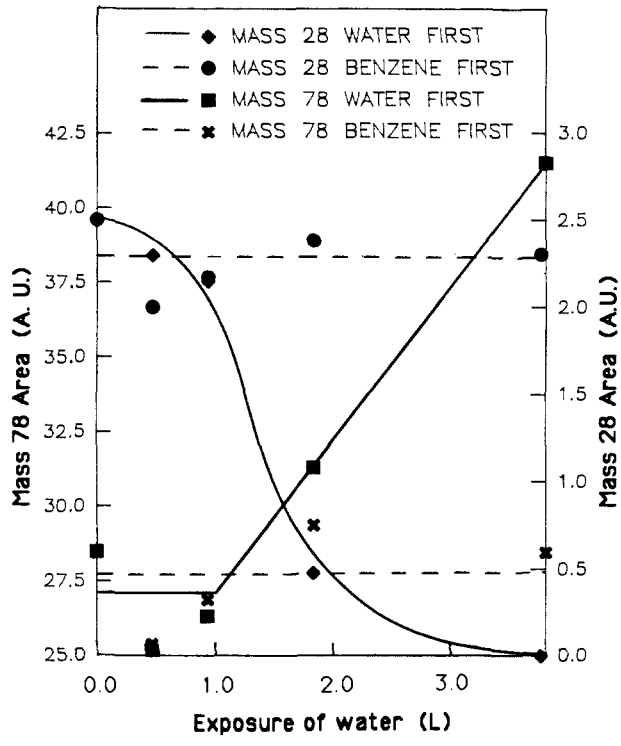

Figure 10. Time-integrated desorption peak areas of CO and benzene, corresponding to coadsorption experiments of the type shown in Figures 9 and 11. Solid lines show results when water is adsorbed first and benzene second, as in Figure 9. Broken lines show results when benzene is adsorbed first and water second, as in Figure 11.

benzene from adsorbing directly at the metal surface.

In Figure 10, the integrated yields of benzene and CO are shown as functions of water exposure (solid lines). The extent of decomposition decreases slowly until, at a water exposure of 1.5 langmuirs, it drops rapidly to zero. At the same time, the amount of molecular benzene which desorbs increases by a factor of 5. Figure 10 illustrates that pre-adsorbed water blocks benzene decomposition while enhancing molecular benzene desorption. [The amount of benzene which desorbs relative to the amount while cracks in the absence of water could be evaluated quantitatively from these data only if the adsorption probability of benzene on water, relative to its value on bare Ru, were known.]

From our other work,[31] it is established that a water exposure of 1.5 langmuirs is necessary and sufficient to completely cover the clean Ru(001) surface with the well-known water bilayer.[33-36] It is therefore reasonable that benzene decomposition drops precipitously to zero after this exposure of water (see Figure 10).

When benzene is adsorbed before water, the amount of decomposition is equal to that which takes place when benzene is adsorbed alone on a clean Ru(001) surface and is independent of water exposure. The amount of molecular desorption is also unchanged, indicating that water cannot displace the benzene from the β-state. This is shown by the dashed lines of Figure 10. The thermal desorption spectra of benzene under these conditions, shown in Figure 11, indicate that water displaces chemisorbed benzene from the α_1 state into the α_2 and α_3 states. That is to say, water displaces the molecular benzene from the weakly chemisorbed sites shown in Figure 7ii into the metastable multilayer and also into the bulk-like multilayer. Since the amount of benzene decomposition is unaffected, this indicates that the desorption process does not compete with the dissociation step. Because water does not influence the extent of decomposition, it

(33) Thiel, P. A.; Hoffmann, F. M.; Weinberg, W. H. *J. Chem. Phys.* **1981**, *75*, 5556.
(34) Doering, D. K.; Madey, T. E. *Surf. Sci.* **1982**, *123*, 305.
(35) Thiel, P. A.; DePaola, R. A.; Hoffmann, F. M. *J. Chem. Phys.* **1984**, *80*, 5326.
(36) Williams, E. D.; Doering, D. L. *J. Vac. Sci.* **1983**, *123*, 305.

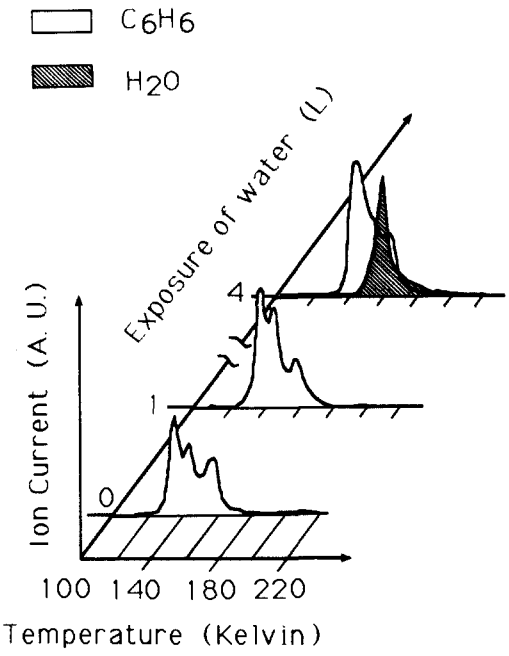

Figure 11. Thermal desorption spectra of benzene (open areas) and water (filled area) following coadsorption at 85 K. The benzene exposure occurs first and water second. Benzene exposures are constant at 0.9 langmuir; water exposures vary.

must be that the fate of an adsorbed benzene molecule—whether it will eventually desorb or dissociate—is fixed by events which occur *at the adsorption temperature, i.e., already at 85 K*, and postadsorbed water cannot reverse this process.

The desorption spectra of water shown in Figures 9 and 11 are strongly perturbed by the coadsorbed benzene. Only a single state is present, at a temperature comparable to that of the normal ice multilayer, at 160 K.[33-35] The two well-defined states of water at higher temperatures, 180 and 220 K, which are characteristic of hydrogen-bonded clusters on *clean* Ru,[33-36] are replaced by a long featureless tail in this temperature range. It may be that the water–water hydrogen bonding which is necessary for formation of the well-ordered surface clusters is disrupted by additional hydrocarbon–water bonding. Hydrogen bonding between water and benzene[37] and also between water and ethylene[38] has been observed in matrix isolation experiments. Also, hydrogen bonding occurs between benzene and hydroxyl groups on Al_2O_3[39] and silica.[40]

(IV) Discussion

Our main result is that between one-half and one-fourth of a full layer of benzene adsorbs *irreversibly* into a β-state upon adsorption at 85 K. All of the molecules which adsorb into the β-phase will eventually dissociate to oxidizable carbon and atomic hydrogen at $T > 500$ K. Therefore, the barrier for adsorption into the β-state is *effectively* the barrier for dissociation, even though the exact nature of the β-state at $T < 500$ K cannot be determined without thorough spectroscopic characterization. The barrier for formation of the β-phase is quite low, since it forms at 85 K; if we assume that the pre-exponential rate factor for β-benzene formation is comparable to that for α_1 desorption, then the upper limit for the energy barrier for β-benzene formation is 9–11 kcal/mol.

Other studies describe only molecular adsorption of benzene up to 300 K on the hexagonal surfaces Ni(111),[1-6] Rh(111),[7,8] Pd(111),[3,11-13,15] and Pt(111)[4,17] as well as the geometrically dissimilar (100) and (110) planes of Ni and Pd.[2,3,5,6,9-11,14-17] [Evidence for some irreversible adsorption is obtained on the stepped surfaces, as well as on the reconstructive Pt(100) surface, however.[5,6,16,17]] We find that desorption of molecular benzene from Ru(001) is complete by 180 K, whereas desorption from Ni, Pd, and Pt occurs between 400 and 550 K.[5,6,8,11,12,15,17] We attribute the lower desorption barrier for Ru to the fact that benzene desorbs from a Ru surface heavily modified by the β-benzene state, whereas on the other metals decomposition appears to *accompany* and *compete with* desorption at higher temperatures.[6,8,11,15,17] One can roughly estimate that the barriers to dissociation and desorption are comparable in the latter case and are about 25–35 kcal/mol on the aforementioned low-index surfaces of Ni, Rh, Pd, and Pt.[45] On the other hand, the upper limit for the *effective* dissociation barrier of benzene on Ru(001) is 9–11 kcal/mol, significantly lower than that for comparable surfaces of Ni, Rh, Pd, or Pt.

Our results are in good agreement with those of Shanahan and Muetterties,[18] who reported irreversible adsorption of benzene on Ru(001) at 300 K and no desorption of molecular benzene following adsorption at 300 K. However, Kelemen and Fischer[19] used photoelectron spectroscopy and concluded that benzene adsorbs without dissociation at 300 K on Ru(001). These two sets of results seem to contradict one another. There are two plausible explanations for this apparent discrepancy. (1) β-Benzene is simply chemisorbed, molecular benzene, even at 300 K. This would account for the photoelectron spectroscopic results of Kelemen and Fischer.[19] However, the chemisorption bond strength of this molecule (which is the energy barrier for desorption) is significantly larger than the energy barrier to dissociation, so that dissociation is the only reaction observed when the surface is heated. This (relatively) strong bond also prevents displacement of β-benzene by chemisorbed water. Such a model would be consistent with all of our results, as well as those of Shanahan and Muetterties.[18] If this model is correct, then the difference between Ru(001) and, for instance, Pt(111) or Ni(111) is primarily in the strength of the chemisorption bond relative to the dissociation barrier. (2) The β phase represents benzene molecules which have undergone dissociation, perhaps even at 85 K, and photoelectron spectroscopy is unable to distinguish molecular benzene from its dissociation products. We note that a dissociation product such as benzyl, which is inferred to exist on supported metal catalysts from isotope exchange data,[42] may not be easily distinguishable from molecular benzene. Acetylene has been observed on supported Rh catalyst following benzene adsorption at 300 K in the presence of CO,[43] which represents another possible decomposition pathway on Ru. If this model is correct, then the difference between Ru and the other metals is that the *actual* barrier to dissociation is much lower on Ru.

These two models cannot be distinguished on the basis of the present data. In either case, however, the effect is the same: benzene adsorbs irreversibly on Ru(001) (even at 85 K) into a phase whose only possible reaction pathway is dissociation.

This issue is an important one for understanding heterogeneous catalysis, since carbonaceous products formed from benzene may be crucial in determining yields and product distributions in hydrogenation and dehydrogenation reactions of cyclic C_6 hydrocarbons over Ru. Recently, Peden and Goodman reported that dehydrogenation of cyclohexane on a Ru(001) crystal reaches steady-state over a carbon-covered surface, and the presence of the carbonaceous overlayer favors dehydrogenation over hydrogenolysis.[45] Similarly, Don and Scholten[46] have reported that the rate of benzene hydrogenation over nonsupported Ru particles decreased slowly with time, presumably due to slow accumulation of decomposition products. Catalyst poisoning could be prevented

(37) Engdahl, A.; Nelander, B. *J. Phys. Chem.* **1985**, *89*, 2861.
(38) Engdahl, A.; Nelander, B. *Chem. Phys. Lett.* **1985**, *113*, 49.
(39) Haalaand, D. M. *Surf. Sci.* **1981**, *102*, 405.
(40) Galkin, G. A.; Kiselev, A. V.; Lygin, V. I. *Trans. Faraday Soc.* **1964**, *60*, 431.
(41) Hoffmann, F. M.; Felter, T. E.; Thiel, P. A.; Weinberg, W. H. *Surf. Sci.* **1983**, *130*, 173.
(42) Moyes, R. B.; Wells, P. B. *Adv. Catal.* **1973**, *23*, 121.
(43) Parker, W. L.; Hexter, R. M.; Siedle, A. R. *J. Am. Chem. Soc.* **1985**, *107*, 4584.
(44) Redhead, P. A. *Vacuum* **1962**, *12*, 203.
(45) Peden, C. H. F.; Goodman, D. W. *J. Catal.*, submitted.
(46) Don, J. A.; Scholten, J. J. F. *Faraday Discuss. Chem. Soc.* **1981**, *71*, 145.

by pre-saturating the powder with water,[46] which is in good agreement with our own observation that pre-adsorbed water prevents benzene decomposition on Ru(001) (Figure 10). Our work indicates that the barrier for benzene dissociation—or, at least, for the irreversible formation of a molecular precursor to dissociation—on ruthenium is unusually low. This may be important for understanding reactions such as benzene hydrogenation or cyclohexane dehydrogenation, in which decomposition products can play a key role.

In summary, we find that between one-half and one-fourth of a full layer of benzene either dissociates or irreversibly forms a molecular precursor to dissociation, upon adsorption at 85 K. This has a strong influence on the coadsorbed benzene which does not dissociate, as evidenced in the thermal desorption spectra. Some benzene chemisorbs weakly (9–11 kcal/mol) at the remaining open metal sites; some forms a metastable multilayer (heat of sublimation = 7 kcal/mol) which grows under the influence of the surface layer; and some desorbs in a normal bulk multilayer (heat of sublimation = 10 kcal/mol). Desorption is complete by 180 K. Water can prevent benzene decomposition but cannot displace benzene from the dissociative phase once it has formed.

Acknowledgments. We thank S.-L. Chang and D. K. Flynn for assistance in the experiments. This research has been supported in part by a Cottrell Research Grant from the Research Corporation, and in part by the Director for Energy Research, Office of Basic Energy Sciences. Ames Laboratory is operated for the U.S. Department of Energy by Iowa State University under Contract No. W-7405-ENG-82. One of us (P.A.T.) is grateful for support of this research via a Fellowship from the Alfred P. Sloan Foundation.

Registry No. Ru, 7440-18-8; C_6H_6, 71-43-2; H_2O, 7732-18-5.

Energy Degradation Pathways and Binding Site Environment of Micelle Bound Ruthenium(II) Photosensitizers

W. J. Dressick,[†] J. Cline, III,[†] J. N. Demas,*[†] and B. A. DeGraff*[‡]

Contribution from the Chemistry Department, University of Virginia, Charlottesville, Virginia 22901, and Chemistry Department, James Madison University, Harrisonburg, Virginia 22807. *Received December 27, 1985*

Abstract: A series of α-diimine Ru(II) sensitizers were studied in aqueous, alcohol, and sodium lauryl sulfate (NaLS) micellar solutions. The emission efficiency, lifetime, and spectra change dramatically on micellization. From the temperature dependence of the excited-state lifetime and luminescence quantum efficiencies, coupled with spectral fitting, we interpret these changes and elucidate the environment of the micellized sensitizer. The increased efficiencies and lifetimes on micellization arise from decreased rates of deactivation via the photoactive d–d state and by a decrease in other intramolecular nonradiative paths. Radiationless decay theory permits semiquantitative calculation of nonradiative rate constants. A model describing the binding site and local solvent environment for the sensitizers is proposed. Implications of the results for solar energy conversion schemes are described.

We are currently studying the photochemistry and photophysics of α-diimine Ru(II) photosensitizers and their interactions in organized media. Our interest is due, in part, to the potential applicability of such systems in solar energy storage schemes.[1-6] Micelles can sequester either reactants or photoproducts and thereby retard energy wasting back reactions.[7-9]

In order to more fully understand the role of organized media in such systems, we have embarked on a systematic study of the photochemistry and photophysics of micellized sensitizers. The Ru(II) sensitizers strongly associate with anionic sodium lauryl sulfate (NaLS) as well as neutral Triton and Brij micelles.[10-16] Upon micellization, significant changes occur in the sensitizer's excited-state lifetime,[10,17-19] luminescence efficiency, and emission band shape.[14,19] These changes reflect the substantial variations in the environment of the emitting metal-to-ligand charge-transfer (MLCT) state on micellization.

We have shown that, especially for NaLS, the Ru(II) sensitizers are tightly micelle bound.[11,16,19] Using the deuterium isotope effect on excited-state lifetimes, we have estimated the degree of aqueous solvent exposure of the bound sensitizers.[16] These results, coupled with earlier $HgCl_2$ quenching results,[11] suggest that sensitizer binding occurs in the Stern layer near the surface of the NaLS micelle.

Although our results leave little doubt as to the binding region in the NaLS micelle, important questions remain concerning the details of the sensitizer's local solvent environment and to what extent it is responsible for the large spectral and lifetime effects

[†] University of Virginia.
[‡] James Madison University.

(1) Calvin, M. *Photochem. Photobiol.* **1983**, *37*, 349.
(2) Fendler, J. H. *J. Phys. Chem.* **1980**, *84*, 1485.
(3) Turro, N. J.; Grätzel, M.; Braun, A. M. *Angew. Chem., Int. Ed. Engl.* **1980**, *19*, 675.
(4) Kalyanasundaram, K. *Chem. Soc. Rev.* **1978**, *7*, 432.
(5) Grätzel, M. *Micellization, Solubilization and Microemulsions*; Mittal, K. L., Ed.; Plenum: New York, 1977; p 531.
(6) Thomas, J. K. *Modern Fluorescence Spectroscopy*; Wehry, E. L., Ed.; Plenum: New York, 1976; p 196.
(7) Takayanagi, T.; Nagamura, T.; Matsuo, T. *Ber. Bunsenges. Phys. Chem.* **1980**, *84*, 1125.
(8) Brugger, P.; Infelta, P. P.; Braun, A.; Grätzel, M. *J. Am. Chem. Soc.* **1981**, *103*, 320.
(9) Nagamura, T.; Kurihara, T.; Matsuo, T. *J. Phys. Chem.* **1982**, *86*, 1886.
(10) Mandal, K.; Hauenstein, B. L.; Demas, J. N.; DeGraff, B. A. *J. Phys. Chem.* **1983**, *87*, 328.
(11) Dressick, W. J.; Hauenstein, B. L.; Demas, J. N.; DeGraff, B. A. *Inorg. Chem.* **1984**, *23*, 1107.
(12) Dressick, W. J.; Raney, K. W.; Demas, J. N.; DeGraff, B. A. *Inorg. Chem.* **1984**, *23*, 875.
(13) Hauenstein, B. L.; Dressick, W. J.; Gilbert, T. B.; Demas, J. N.; DeGraff, B. A. *J. Phys. Chem.* **1984**, *88*, 1902.
(14) Dressick, W. J.; Demas, J. N.; DeGraff, B. A. *J. Photochem.* **1984**, *24*, 45.
(15) Dressick, W. J.; Hauenstein, B. L.; Gilbert, T. B.; Demas, J. N.; DeGraff, B. A. *J. Phys. Chem.* **1984**, *88*, 3337.
(16) Hauenstein, B. L.; Dressick, W. J.; Buell, S. L.; Demas, J. N.; DeGraff, B. A. *J. Am. Chem. Soc.* **1983**, *105*, 4251.
(17) Atherton, S. J.; Baxendale, J. H.; Hoey, B. M. *J. Chem. Soc., Faraday Trans. 1* **1982**, *78*, 2167.

0002-7863/86/1508-7567$01.50/0